Gastrointestinal System

15

Esophageal Transit Study (Tc-99m-Sulfur Colloid in Water)

Overview The images of the Esophageal Motility Study demonstrate the movement of a bolus of swallowed material through the esophagus and into the stomach in a physiologic and quantitative fashion [1, 2].

Radiopharmaceutical characteristics The radiopharmaceutical consists of Tc-99m-sulfur colloid mixed in water. The size of the colloidal particles covers a wide range from 0.03 to 10 μm. Most particles are in the 0.4–0.8 μm range [3].

Extraction mechanism None. The Tc-99m-sulfur colloid remains in the esophagogastric lumen.

Extraction efficiency Zero percent.

Extraction mechanism saturable or non-saturable Not applicable.

Interventions None.

Imaging Imaging is performed with a dual-head gamma camera with low-energy high-resolution parallel-hole collimators.

Protocol design The patient lies in the supine position, imaging is performed with a dual-head gamma camera, and images are acquired in the anterior and posterior projections. The patient is instructed to swallow a 15 mL aliquot of the radiopharmaceutical in a single bolus and to follow this with dry swallows (no liquid) every 15 s for up to 10 min. Anterior and posterior digital images are acquired beginning when the patient swallows the radiopharmaceutical. The images are acquired for 1 s each for the first 15 s and then for 15 s each for up to 10 min (Fig. 15.1) [1, 2].

Quantitative measurement Evaluation of esophageal transit time is an example of a relative quantitative measurement (see Chap. 8, Quantitation of Function: Relative Measurements). The esophageal transit time is a relative measurement because multiple data points are generated over time from the same region of inter-

W.C. Klingensmith III, *The Mathematics and Biology of the Biodistribution of Radiopharmaceuticals-A Clinical Perspective*,
DOI 10.1007/978-3-319-26704-3_15

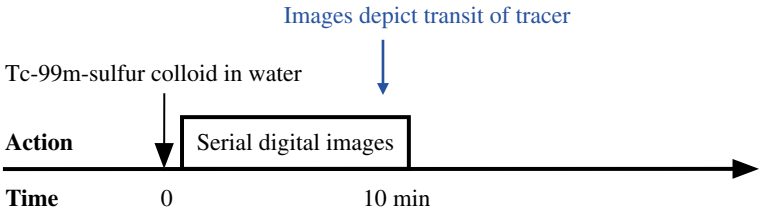

Fig. 15.1 Protocol summary diagram

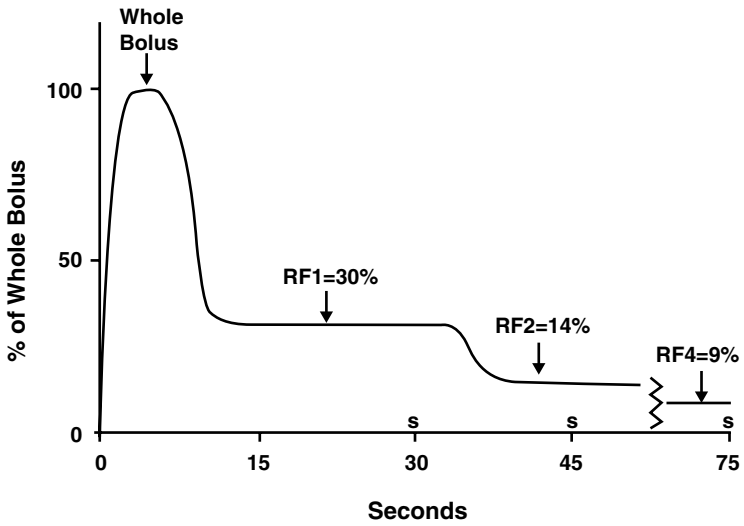

Fig. 15.2 Time-activity curve from esophageal transit study. The peak time, "whole bolus," represents the total amount of radiopharmaceutical that was administered. "RF" is the residual fraction of tracer in the esophagus after each swallow [1]

est (ROI). The measurements are not related to the amount administered radiopharmaceutical. No background subtraction is needed because the activity is limited to the organ of interest, the esophagus.

A ROI is drawn over the esophagus excluding the stomach in the anterior and posterior images. The geometric mean of the activity in the anterior and posterior images at each time point is calculated. The geometric mean process compensates for attenuation in a relative fashion (see Chap. 8, Quantitation of Function: Relative Measurements). The data can be displayed in multiple ways, but an esophageal emptying curve depicting the residual tracer in the esophagus similar to the gastric emptying curve is most convenient (Fig. 15.2).

The esophageal time-activity curve can be analyzed in various ways, but it is usually evaluated by calculating the meant transit time [2–5]. The upper limits for the mean transit time of esophageal emptying is 10 s [5].

Gastric Emptying Study (Tc-99m-Sulfur Colloid in Instant Oatmeal)

Overview The images of the Gastric Emptying Study demonstrate the movement of an ingested bolus of a labeled meal through the stomach into the small intestine. Various physiologic parameters may be quantified, but the most important parameter is the rate of emptying of the test meal. A wide variety of meals and protocols have been published and are in clinical use [6–10]. Here, we will focus on the relatively simple meal of instant oatmeal labeled with Tc-99m-sulfur colloid [10, 11].

Radiopharmaceutical characteristics Technetium-99m is firmly bound to sulfur colloid, which in turn binds to the contents of one packet of instant oatmeal. The Tc-99m-sulfur colloid should be added to the oatmeal before it is reconstituted with hot water to achieve optimal binding of the tracer to the instant oatmeal [7]. The reconstituted oatmeal is considered a semisolid meal. Compared to a solid meal a semisolid meal has the advantage that it can be ingested more quickly and produce a more defined start time.

Extraction mechanism None. The labeled oatmeal remains in the gastrointestinal lumen.

The radiopharmaceutical bolus moves through the stomach by peristalsis, which is under both neural and hormonal control. The neural control system has both an extrinsic component, the vagus nerve, and an intrinsic component consisting of several neural plexi within the gastric wall (Fig. 15.3) [12].

Extraction efficiency Zero percent.

Extraction mechanism saturable or non-saturable Not applicable.

Interventions In general, none [13].

Imaging Imaging is performed with a dual-head gamma camera with low-energy parallel-hole collimators.

Protocol design The patient is instructed to eat the oatmeal meal in less than 5 min. Then anterior and posterior images of the upper abdomen are acquired immediately and every 15 min for 1 h with the patient standing (Fig. 15.4). Delayed images are acquired if necessary.

Quantitative measurement The primary information from the Gastric Emptying Study is a quantitative measurement of the transit time of a labeled semisolid meal through the stomach.

The gastric emptying time is a relative measurement because the data is generated over time from the same anterior and posterior ROIs (see Chap. 8, Quantitation of Function: Relative Measurements). No background subtraction is needed because the activity is limited to the organ of interest, the stomach.

The geometric mean of the activity in the anterior and posterior images at each time point is calculated. The geometric mean process compensates for attenuation in a relative fashion. The data can be analyzed in multiple ways, but most commonly the half time of emptying is used [14]. The mean transit time could also be used and, in most cases, would give similar, but not identical, results.

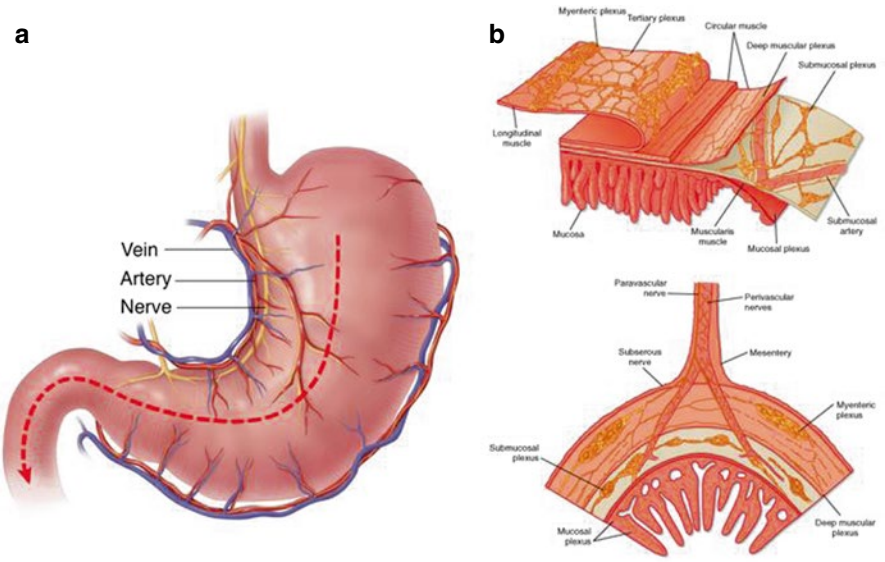

Fig. 15.3 (**a**, **b**) Anatomy and intrinsic myenteric plexi of the stomach. Gastric meals move through the stomach under hormonal and neural control. The neural system has both extrinsic (vagus nerve) and intrinsic (myenteric neural system) components [12]

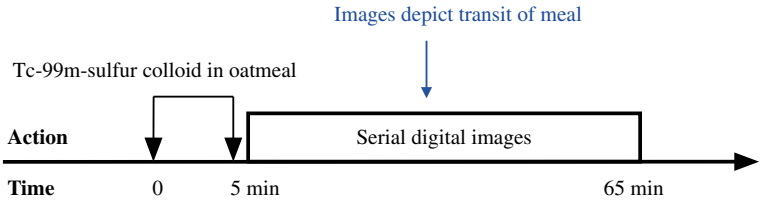

Fig. 15.4 Protocol summary diagram

The upper limits of normal for the half time of emptying of one packet of instant oatmeal vary with age (Table 15.1) [11]. The reproducibility of the gastric emptying study with an oatmeal meal also varies with age (Table 15.1).

Gastrointestinal Bleeding Study (Tc-99m-Red Blood Cells)

Overview The images of the Gastrointestinal Bleeding Study detect the extravasation of radiolabeled red blood cells from the vascular space into the gastrointestinal lumen. The subsequent movement of the extravasated red blood cells within the gastrointestinal lumen secondary to peristalsis allows localization of the site of bleed along the gastrointestinal tract [15, 16].

Table 15.1 Proposed and (actual) normal limits for gastric emptying times and reproducibility

	Normal range (min)		Reproducibility (min)	
Sex and age	LAO	A-P	LAO	A-P
Males and females				
20–40 years				
Proposed	10–60	10–60	≤30	≤30
Mean ± 2 sd	(0–62)	(0–67)	(0–34)	(0–39)
Range	(20–60)	(13–56)	(4–27)	(8–35)
40–60 years				
Proposed	10–40	10–40	≤20	≤20
Mean ± 2 sd	(0–52)	(0–50)	(0–22)	(0–19)
Range	(9–44)	(12–42)	(1–18)	(0–18)
60–80 years				
Proposed	10–30	10–30	≤15	≤15
Mean ± 2 sd	(0–30)	(0–28)	(0–22)	(0–15)
Range	(9–26)	(15–26)	(2–18)	(0–13)

Radiopharmaceutical characteristics The Tc-99m-red blood cell is one of the largest radiopharmaceuticals with a diameter of approximately 8 μm, a thickness of approximately 2 μm, and a central thickness of approximately 1 μm [17].
Extraction mechanism None. The Tc-99m-red blood cells are confined to the vascular space except when there is a gastrointestinal bleed, in which case the compartment that the Tc-99m-red blood cells occupy is effectively enlarged.
Extraction efficiency Not applicable.
Extraction mechanism saturable or non-saturable Not applicable.
Imaging Imaging is performed with a gamma camera and a low-energy high-resolution parallel-hole collimator [18].
Interventions None.
Protocol design Beginning at the time of injection of the radiopharmaceutical serial 1 min images are obtained. Every 30 min, the previous set of 30 images is reviewed in cine mode by the nuclear medicine physician while the next 30 min collection is started. This process is continued until: (1) a bleeding site is identified and localized, (2) the patient refuses further imaging, (3) the gamma camera is needed for another study, (4) the patient is needed elsewhere for another study, or (5) the nuclear medicine physician terminates the imaging session. Imaging can be restarted the following day. One injection of radiopharmaceutical allows imaging for up to 36 h (Fig. 15.5).
Quantitative measurement None.

Hepatic Artery Perfusion Study (Tc-99m-Macroaggregated Albumin)

Overview The images of the Hepatic Artery Perfusion Study depict the distribution of perfusion, actually clearance, via an hepatic artery catheter. The catheter is usually placed so that the injected tracer distributes to only one lobe of the liver.

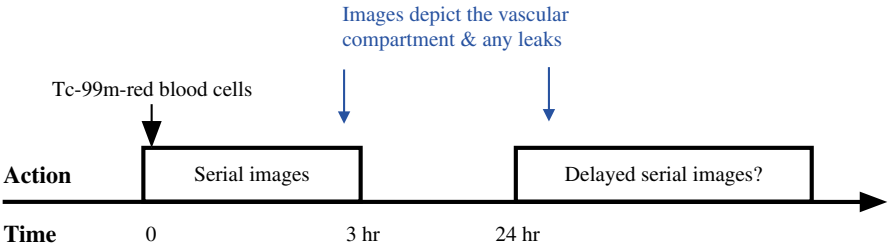

Fig. 15.5 Protocol summary diagram

However, if the catheter is not optimally placed, the tracer may go to both lobes and some tracer may go to the stomach or other extrahepatic locations.

In addition, if there are anatomic arteriovenous shunts within the liver, some Tc-99m-MAA will pass through the liver and embolize in the lung capillaries. The percent of Tc-99m-MAA that passes through the liver and lodges in the lungs can be quantified [19]. If excessive amounts of radiopharmaceutical reach the lungs, the amount of injected dose is reduced or the procedure is canceled.

Radiopharmaceutical characteristics Ninety percent of Tc-99m-macroaggregated particles range in size from 10 to 80 μm with a mean particle size of 30 μm. No particles exceed 150 μm [20].

Extraction mechanism Following intracatheter injection, the particles will embolize into arterioles of the first capillary bed they encounter.

However, the particles will pass through anatomic arteriovenous shunts. Thus, this radiopharmaceutical distributes according to clearance and is removed from flowing blood by microembolization into capillary beds. Even though there is very high blood flow through intrahepatic anatomic arteriovenous shunts, there will be very little localization or clearance of Tc-99m-macroaggregated in these structures. This fact demonstrates the inaccuracy of calling this study a perfusion study. This is another example of the use of clearance as a proxy for blood flow.

In the liver, the clearance of Tc-99m-macroaggregated will reflect blood flow except where there are intrahepatic arteriovenous shunts. Generally, the presence of the tracer in the lungs indicates the presence of intrahepatic arteriovenous shunts.

Extraction efficiency Essentially 100 % for arterioles and capillary beds.

Extraction mechanism saturable or non-saturable Not saturable.

Interventions None.

Imaging Imaging is initially performed with a gamma camera with a low-energy high-resolution parallel-hole collimator followed by imaging with a SPECT-CT machine [21].

Protocol design Following injection of the Tc-99m-macroaggregated albumin, anterior and posterior images of the lungs and upper abdomen are acquired. Then SPECT-CT images are obtained of the upper abdomen (Fig. 15.6).

Quantitative measurement The images are used to calculate the percent of Tc-99m-macroaggregated albumin that passed through the liver and embolized into the pulmonary capillary beds. This percentage is used to adjust the dose of

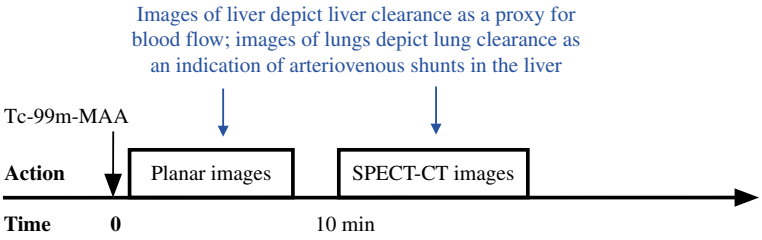

Fig. 15.6 Protocol summary diagram

Table 15.2 Dose reduction for intrahepatic shunting

Intrahepatic shunting (%)	Reduction percent
<10	No reduction
10–15	20 % reduction
15–20	40 % reduction
>20	No treatment

Y-90-spheres that can be injected for treatment of cancer in the liver [22]. Because of the possibility of radiation damage to the lungs, a moderate amount of shunting of Tc-99m-macroaggregated albumin to the lungs requires a moderate reduction in the dose of the Y-90-spheres and a large amount of shunting requires cancellation of the therapy (Table 15.2) [22].

The intrahepatic arteriovenous shunt determination represents a relative quantitative measurement in that one ROI of a part of the body is compared to another at the same point in time, but not to the amount of activity injected (see Chap. 8, Quantitation of Activity: Relative Measurements). Because the radiopharmaceutical is injected into the hepatic catheter, the activity is essentially limited to the liver and lungs, so no background correction is needed.

The geometric mean of the counts in the lungs and liver is calculated to account for attenuation in a relative fashion. ROIs are placed over these organs in the anterior and posterior images, the opposing counts are multiplied together, and then the square root is obtained. However, the geometric mean approach to compensating for attenuation is exact only when the density of tissue in all of the ROIs is the same, which is not the case for the lungs and the liver. For practical reasons, this limitation is ignored.

The applicable equation is,

$$\mathrm{IHAVS}(\%) = \frac{\left[L_{\mathrm{Ant}}(\mathrm{cpm}) \times L_{\mathrm{Post}}(\mathrm{cpm})\right]^{1/2}}{\left[\left[L_{\mathrm{Ant}}(\mathrm{cpm}) + H_{\mathrm{Ant}}(\mathrm{cpm})\right] \times \left[L_{\mathrm{Post}}(\mathrm{cpm}) + H_{\mathrm{Post}}(\mathrm{cpm})\right]\right]^{1/2}} \times 100(\%) \tag{15.1}$$

where "IHAVS" is intrahepatic arteriovenous shunt as a percent, L is both the lungs and H is the liver in counts per minute, and "Ant" and "Post" are the anterior and posterior projections.

Table 15.2 lists the algorithm for reducing the dose of Y-90-spheres (SIRTeX) for varying degrees of intrahepatic arteriovenous shunting [22].

Hepatic Hemangioma Study (Tc-99m-Red Blood Cells)

Overview The images of the Hepatic Hemangioma Study depict the amount of blood flow (early images) and vascular space (delayed images) within hepatic lesions. Hemangiomas are characterized by their relatively decreased blood flow and increased vascular volume compared to hepatic parenchyma and most other hepatic lesions [23].
Radiopharmaceutical characteristics The Tc-99m-red blood cell is one of the largest radiopharmaceuticals with a diameter of approximately 8 μm, a thickness of approximately 2 μm, and a central thickness of approximately 1 μm [17].
Extraction mechanism None. The Tc-99m-red blood cells are confined to the vascular space except when there is a gastrointestinal bleed, in which case the compartment that the Tc-99m-red blood cells occupy is effectively enlarged.
Extraction efficiency Zero percent.
Extraction mechanism saturable or non-saturable Not applicable.
Imaging Imaging is performed with a gamma camera with a low-energy high-resolution parallel-hole collimator.
Interventions None.
Imaging Images are acquired with a dual-headed SPECT gamma camera or SPECT-CT.
Protocol design Immediately following injection of the radiopharmaceutical, serial planar images of the liver are acquired for 90 s to evaluate blood flow to the lesion in question. Then static planar images of the liver are acquired in the anterior, posterior, right lateral, and left lateral projections. Finally, SPECT-CT images of the upper abdomen are acquired (Fig. 15.7).
Quantitative measurement None.

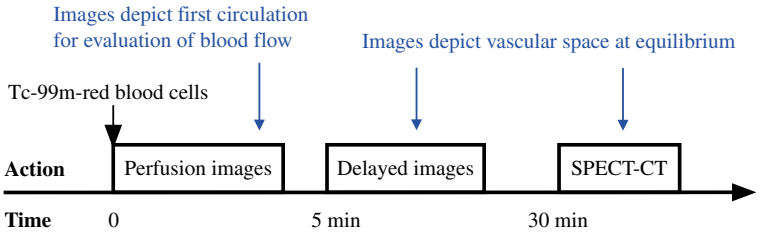

Fig. 15.7 Protocol summary diagram

Hepatobiliary Study (Tc-99m-Trimethylbromo-IDA)

Overview The images of the Hepatobiliary Study successively demonstrates hepatocyte clearance, hepatic parenchymal transit, and biliary excretion as the radiopharmaceutical moves from the injection site into the hepatobiliary system, through the intrahepatic bile ducts, and into the extrahepatic biliary system. In addition, the gallbladder ejection fraction is measured [24, 25].

Radiopharmaceutical characteristics The chemical structure of Tc-99m-trimethylbromo-IDA is shown in Fig. 15.8. It has a molecular weight of 408.18.

Extraction mechanism Following intravenous injection, Tc-99m-trimethylbromo-IDA reaches the sinusoids of the liver via the hepatic artery and portal vein where it is transported (cleared) into the hepatocytes via a system that excretes a class of relatively small organic anions. The mechanism of transporting the radiopharmaceutical across the sinusoidal membrane of the hepatocyte is not completely known, but may be passive diffusion along a radiopharmaceutical gradient [26, 27]. Once the radiopharmaceutical reaches the canalicular membrane of the hepatocyte, the tracer is actively transported by the multidrug resistance-associated protein (MRP2) from the hepatocyte into the bile canaliculus (Fig. 15.9) [28]. Thus, Tc-99m-trimethylbromo-IDA is one of a class of molecules that is excreted by the hepatobiliary excretory system.

Extraction efficiency Moderate-high, imaging begins at 15 min.

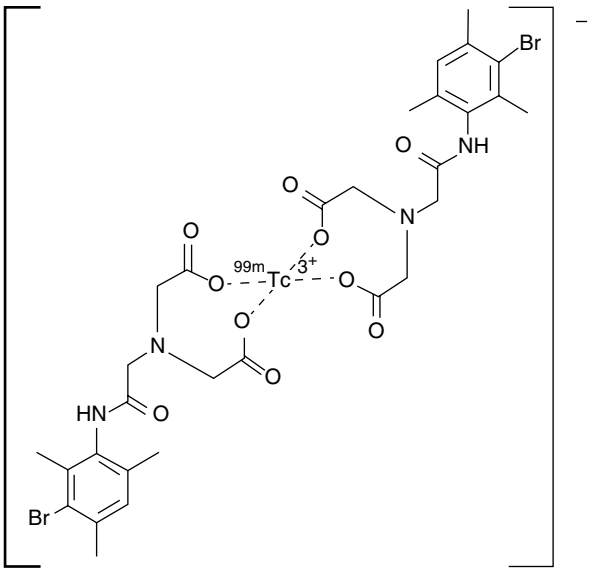

Fig. 15.8 Chemical structure of Tc-99m-trimethylbromo-IDA

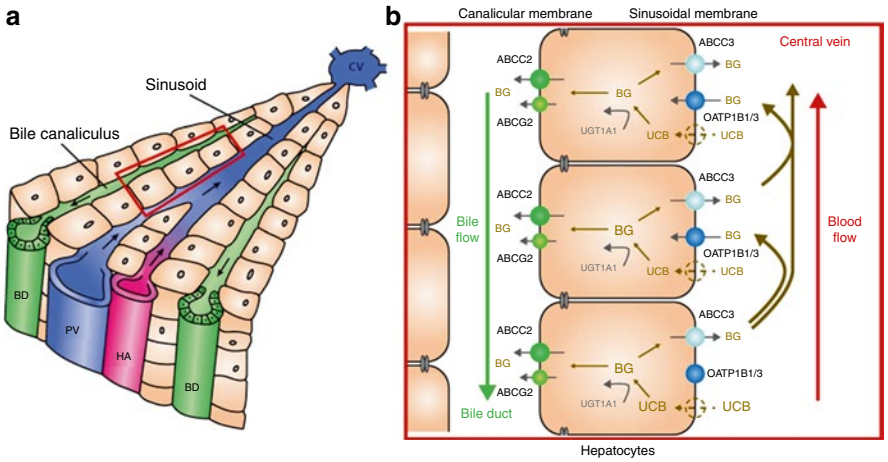

Fig. 15.9 Cellular biology of excretion of Tc-99m-trimethylbromo-IDA through the bilirubin excretion pathway. (**a**) Liver lobule: *BD* bile duct, *PV* portal vein, *HA* hepatic artery, *CV* central vein. (**b**) Unconjugated bilirubin (*UCB*) enters hepatocytes via passive diffusion and/or transporters. Tc-99m-trimethylbromo-IDA follows the same excretory pathway as bilirubin, but is not conjugated (van de Steeg et al. [27], fig 6)

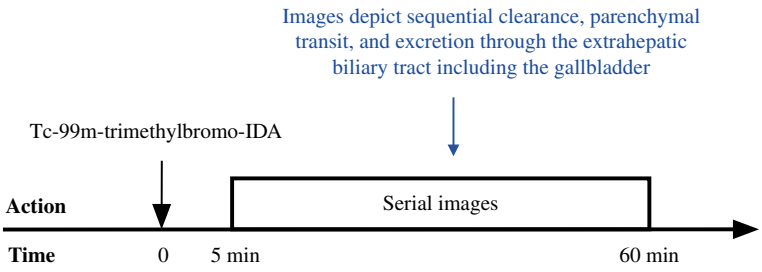

Fig. 15.10 Protocol summary diagram

Extraction mechanism saturable or non-saturable Saturable. Bilirubin is a competing molecule.

Interventions Kinevac, an analog of cholecystokinin, is frequently used to evaluate contraction of the gallbladder, and morphine can be used to cause closure of the sphincter of Oddi in order to enhance visualization of the gallbladder [29, 30].

Imaging Imaging is performed with a dual-headed gamma camera with a low-energy high-resolution parallel-hole collimator.

Protocol design Images are acquired in the anterior and right lateral projections beginning 5 min after injection through 60 min (Fig. 15.10) [24, 25].

Quantitative measurement (visual): Parenchymal transit time Radiopharmaceutical should appear in the extrahepatic biliary tract (usually the left or right hepatic ducts, but sometimes the gallbladder) by 15 min from injection of the radiopharmaceutical [24, 25].

Quantitative measurement: Gallbladder ejection fraction Assuming that the gallbladder is reasonably well visualized at the end of routine imaging at 60 min, the gallbladder ejection fraction can be measured in response to a 30 min infusion of Kinevac (analog of cholecystokinin) [30–33]. The 60 min anterior image from the routine image set is used as the pre-Kinevac baseline image of the gallbladder. After the 30 min infusion of Kinevac, another anterior image is obtained.

Since there is little change in photon attenuation between the end-diastolic and end-systolic images of the left gallbladder, and since the gallbladder ejection fraction is a relative measurement, there is no need to know the absolute amount of activity in the gallbladder, and attenuation correction can be ignored.

However, since there is significant activity in the tissues around the gallbladder, background correction is needed. The background ROI is placed medial to the gallbladder and must not overlap the gallbladder. The equation for background correction of an ROI is given in Eqs. 8.8 and 8.7 of Chap. 8, Quantitation of Function: Relative Measurement.

The equation for the gallbladder ejection fraction, after the pre- and post-Kinevac gallbladder ROIs are corrected for background activity, is simply

$$GB_{EF}(\%) = \frac{GB_{Pre}(\text{cpm}) - GB_{Post}(\text{cpm})}{GB_{Pre}(\text{cpm})} \times 100(\%) \tag{15.2}$$

Here, "GB_{EF} (%)" is the gallbladder ejection fraction in percent, "GB_{Pre} (cpm)" is the background-corrected counts per minute in the pre-Kinevac gallbladder, and "GB_{Post} (cpm)" is the background-corrected counts per minute in the post-Kinevac gallbladder.

Gallbladder ejection fraction: Normal range The lower limits of normal for gallbladder ejection fraction following a 30 min infusion of Kinevac is 30 % [31].

Liver-Spleen Study

Overview The images of the Liver/Spleen Study demonstrate the distribution of the intravascular mononuclear phagocyte (macrophage) system. The intravascular members of this cell system line the sinusoids of the liver (Kupffer cells), spleen, and bone marrow.

Radiopharmaceutical characteristics Tc-99m-sulfur colloid consists of the colloidal particles covering a wide range in size from 0.1 to 2 μm. Most particles are in the 0.4–0.8 μm range [34, 35].

Extraction mechanism Tc-99m-sulfur colloid and similar particles are removed from the circulation by macrophages via phagocytosis (Fig. 15.11) [36, 37].

Macrophages are large white blood cells which temporarily occlude capillary lumens until they are able to deform, pass through the capillary, and reenter the flowing blood in the venule. Thus, in most capillary beds, macrophages cannot phagocytose particles from blood flowing past them. However, in sinusoids the

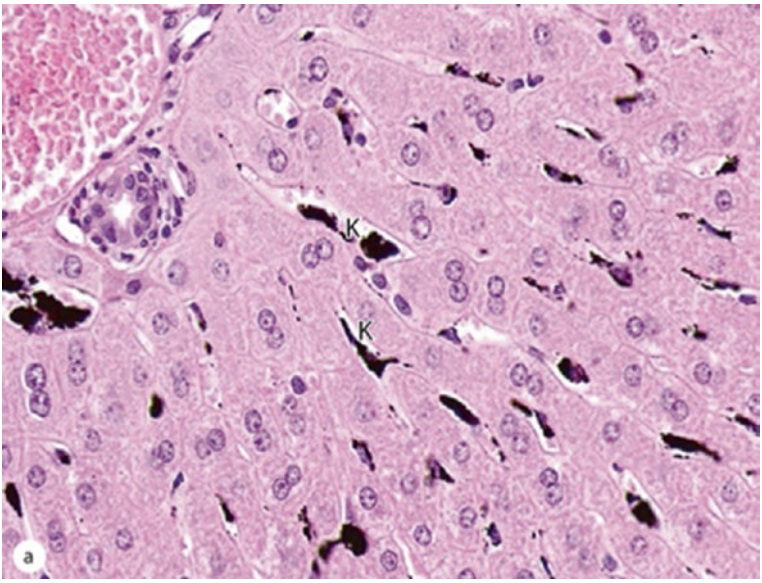

Fig. 15.11 Histologic image of rat liver following intravenous injection of particulate India ink. The Kupffer cells (macrophages) in the sinusoids (K) contain large amounts of particulate India ink. Notice that the Kupffer cells line the margins of the sinusoids and do not obstruct flow. Any circulating particles flow past the Kupffer cells and make contact with the pseudopods extending from the plasma membrane initiating phagocytosis (Junqueira's *Basic Histology: Text and Atlas*. Lange & McGraw Hill Mescher AL, 2013, p 336, fig 16-15)

lumen is larger than in ordinary capillaries, and macrophages can assume a marginal position without obstructing flow. Here colloidal particles brush up along the macrophages and are phagocytized.

Phagocytosis is a triggered process. The colloidal particles bind to the macrophages and initiate the process of invagination, the creation of a phagosome around the colloid, and the internalization of the phagosome by the macrophage.

Extraction efficiency High. At 5 min after intravenous injection of the Tc-99m-sulfur colloid, essentially all of the radiopharmaceutical has been cleared from the blood and imaging can begin. Normally, 80–85 % of the dose localizes in the liver, 5–10 % in the spleen, and the rest in the bone marrow [38].

Extraction mechanism saturable or non-saturable Non-saturable.

Interventions None.

Imaging Imaging is performed with a dual-headed gamma camera with a low-energy high-resolution parallel-hole collimator.

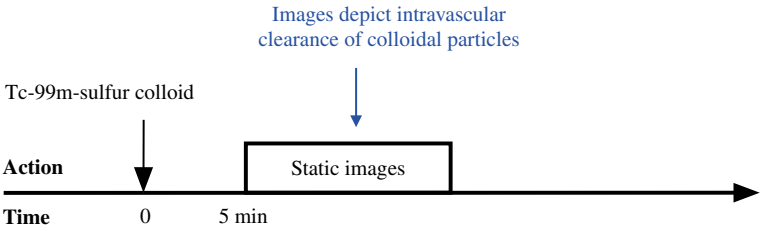

Fig. 15.12 Protocol summary diagram

Protocol design Anterior and posterior images are obtained of the upper abdomen in the anterior and posterior projections and in both lateral projections (Fig. 15.12).
Quantitative measurement None.

Meckel's Diverticulum Study (Tc-99m-Pertechnetate)

Overview The images of the Meckel's Diverticulum Study depict the uptake of pertechnetate within the abdomen. Pertechnetate is secreted by the mucosa of the stomach as well as by any ectopic gastric mucosa. Because pertechnetate exhibits only weak protein binding, it is also filtered by the kidneys.
Radiopharmaceutical characteristics The chemical structure of Tc-99m-pertechnetate is shown in Fig. 15.13. It has a molecular weight of 162.91.
Extraction mechanism Autoradographic evidence suggests that in the stomach, Tc-99m-pertechnetate is primarily secreted by the mucous producing epithelial cells [36, 37].
Extraction efficiency Moderate.
Extraction mechanism saturable or non-saturable Intravenous administration of perchlorate can compete with Tc-99m-pertechnetate, but this is rarely a clinical problem [36, 37].
Interventions There is some evidence that cimetidine can enhance the secretion of Tc-99m-pertechnetate [39, 40].
Imaging Images are acquired with a dual-head gamma camera fitted with a low-energy, high-resolution, parallel-hole collimator.
Protocol design Serial anterior and posterior static images are obtained for 1 h following injection of the Tc-99m-pertechnetate (Fig. 15.14).
Quantitative measurement None.

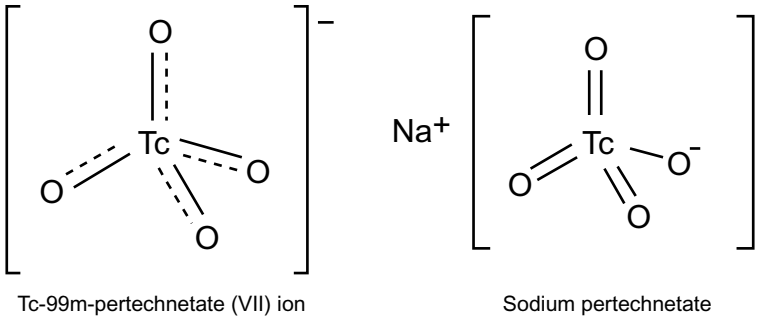

Fig. 15.13 Chemical structure of sodium pertechnetate

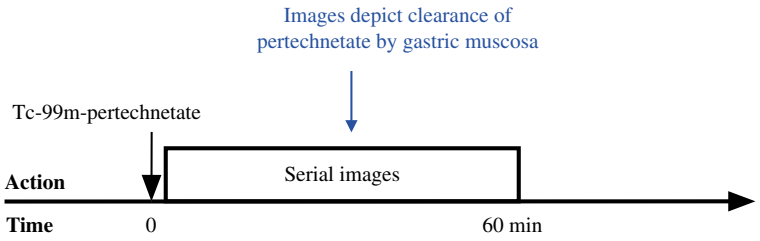

Fig. 15.14 Protocol summary diagram

References

Esophageal Transit Study (Tc-99m-Sulfur Colloid in Water)

1. Klein HA. Esophageal transit scintigraphy. Semin Nucl Med. 1995;25:306–17.
2. Mariani G, Boni G, Barreca M, et al. Radionuclide gastroesophageal motor studies. J Nucl Med. 2004;45:1004–28.
3. Eshima D, Eshima L, Gotti NM, et al. Technetium-99m-sulfur colloid for lymphoscintigraphy: effects of preparation parameters. J Nucl Med. 1996;37:1575–8.
4. Tatsch K, Voderholzer WA, Weiss MJ, et al. Reappraisal of quantitative esophageal scintigraphy by optimizing results with ROC analyses. J Nucl Med. 1996;37:1799–805.
5. Jorgensen F, Hesse B, Tromholt N, et al. Esophageal scintigraphy: reproducibility and normal ranges. J Nucl Med. 1992;33:2106–9.

Gastric Emptying Study (Tc-99m-Sulfur Colloid Labeled Oatmeal)

6. Fitzpatrick ML, Alderson AM. Solid food label for measurement of gastric emptying [Letter]. Br J Radiol. 1979;52:920–1.
7. Maloy TA, Herrera M, Zimmer M, et al. Optimal radiolabeling methods for Tc-99m-sulfur colloid oatmeal products for gastric emptying. J Nucl Med. 2011;52:498.
8. Abell TL, Camilleri M, Donohoe K, et al. Consensus recommendations for gastric emptying scintigraphy: a joint report of the American Neurogastroenterology and Motility Society and

the Society of Nuclear Medicine. Am J Gastroenterol. 2008;103:753–63 & J Nucl Med Technol. 2008;36:44–54.
9. Gryback P, Hermansson G, Lyrenas E, et al. Nationwide standardization and evaluation of scintigraphic gastric emptying: reference values and comparisons between subgroups in a multicenter trial. Eur J Nucl Med. 2000;27:647–55.
10. Klingensmith WC, Lawrence SP. The gastric emptying study: protocol design considerations. J Nucl Med Technol. 2008;36:195–9.
11. Klingensmith WC, Rhea KL, Wainwright EA, et al. The gastric emptying study with oatmeal: normal range and reproducibility as a function of age and sex. J Nucl Med Technol. 2010;38:186–90.
12. Koeppen BM, Stranton BA. Berne and Levy physiology. 6th ed. Mosby/Elsevier: Philadelphia; 2008, fig. 26–8, p. 494.
13. Urbain JLC, Vantrappen G, Janssens J, et al. Intravenous erythromycin dramatically accelerates gastric emptying in gastroparesis diabeticorum and normals and abolishes the emptying discrimination between solids and liquids. J Nucl Med. 1990;31:1490–3.
14. Ziessman HA, Atkins FB, Vemulakonda US, et al. Lag phase quantification for solid gastric emptying studies. J Nucl Med. 1996;37:1639–43.

Gastrointestinal Bleeding Study (Tc-99m-red Blood Cells)

15. Winzelberg GG, McKusick KA, Froelich JW, et al. Detection of gastrointestinal bleeding with Tc-99m-labeled red blood cells. Semin Nucl Med. 1982;12:139–46.
16. Zuckier LS. Acute gastrointestinal bleeding. Semin Nucl Med. 2003;33:297–311.
17. Freedman JC. Cell membranes. In: Sperelakis N, editor. Cell physiology sourcebook: essentials of membrane biophysics. 4th ed. London: Academic; 2012. p. 49.
18. Yama N, Ezoe E, Kimura Y, et al. Localization of intestinal bleeding using a fusion of Tc-99m-labeled RBC SPECT and x-ray CT. Clin Nucl Med. 2005;30:488–9.

Hepatic Artery Perfusion Study (Tc-99m-Macroaggregated Albumin)

19. Giammarile F, Bodei L, Chiesa C, et al. EANM procedure guideline for the treatment of liver cancer and liver metastases with intra-arterial radioactive compounds. Eur J Nucl Med. 2011;38:1393–406.
20. Hunt AP, Frier M, Johnson RA, et al. Preparation of Tc-99m-macroaggregated albumin from recombinant human albumin for lung perfusion imaging. Eur J Pharm Biopharm. 2006;62:26–31.
21. Hamami ME, Poeppel TD, Muller S, et al. SPECT-CT with Tc-99m-MAA in radioembolization with Y-90 microspheres in patients with hepatocellular cancer. J Nucl Med. 2009;50:688–92.
22. SIR-Spheres microspheres (Yittrium-90 Microspheres) Package insert. Wilmington: Sirtex Medical Inc.

Hepatic Hemangioma Study (Tc-99m-Red Blood Cells)

23. Schillaci O, Danieli R, Manni C, et al. Technetium-99m-labelled red blood cell imaging in the diagnosis of hepatic haemangiomas: the role of SPECT/CT with a hybrid camera. Eur J Nucl Med Mol Imaging. 2004;31:1011–5.

Hepatobiliary Study (Tc-99m-Trimethylbromo-IDA)

24. Klingensmith WC. Hepatobiliary imaging: normal appearance and normal variations. In: Gottschalk A, Hoffer PA, Berger HJ, Potchen EJ, editors. Diagnostic nuclear medicine. Baltimore: Williams and Wilkins; 1988.
25. Klingensmith WC, Spitzer VM, Fritzberg AR. The normal fasting and postprandial Tc-99m-diisopropyl-IDA hepatobiliary study. Radiol. 1981;141:771–6.
26. Kamisako T, Kobayashi Y, Takeuchi K, et al. Recent advances in bilirubin metabolism research: the molecular mechanism of hepatocyte bilirubin transport and its clinical relevance. J Gastroenterol. 2000;35:659–64.
27. van de Steeg E, Stranecky V, Hartmannova H, et al. Complete OAT1B1 and OATP1B3 deficiency causes human Rotor syndrome by interrupting conjugated bilirubin reuptake into the liver. J Clin Invest. 2012;122:519–28.
28. Jedlitschky G, Keier I, Hummel-Eisenbeiss J, et al. ATP-dependent transport of bilirubin glucronides by the multidrug resistance protein MRP1 and its heptocyte canalicular isoform MRP2. Biochem J. 1997;327:305–10.
29. Chen CC, Holder LE, Maunoury C, et al. Morphine augmentation increases gallbladder visualization in patients pretreated with cholecystokinin. J Nucl Med. 1997;38:644–7.
30. Ziessman HA, Fahey FH, Hixson DJ. Calculation of a gallbladder ejection fraction: advantage of continuous sincalide infusion over the three-minute infusion method. J Nucl Med. 1992;33:537–41.
31. Ziessman HA, Muenz L, Agarwal AK, et al. Normal values for sincalide cholescintigraphy: comparison of two methods. Radiol. 2001;221:404–10.
32. Xynos E, Pechlivanides G, Zoras OJ, et al. Reproducibility of gallbladder emptying scintigraphic studies. J Nucl Med. 1994;35:835–9.
33. Pons V, Sopena R, Hoyos M, et al. Quantitative cholescintigraphy: selection of random dose for CCK-33 and reproducibility of abnormal results. J Nucl Med. 2003;44:446–50.

Liver-Spleen Study (Tc-99m-Sulfur Colloid)

34. Klingensmith WC, Spitzer VM, Fritzberg AR, et al. Normal appearance and reproducibility of liver-spleen studies with Tc-99m-sulfur colloid and Tc-99m-microalbumin colloid. J Nucl Med. 1983;24:8–13.
35. Karesh S. Radiopharmaceuticals in nuclear medicine: consultants in nuclear medicine. www.nucmedtutorials.com/dwradiopharm/rad9.html.
36. Intracellular vesicular traffic. In: Alberts B, Johnson A, Lewis J, et al., editors. The molecular biology of the cell, 5th ed. New York, NY: Garland Science; 2008. p. 787–98.
37. Saha GB. Diagnostic uses of radiopharmaceuticals in nuclear medicine. In: Saha GB, editor. Fundamentals of nuclear pharmacy. 6th ed. New York: Springer; 2010.
38. Hindie E, Coals-Linhart N. Microautoradiographic study of technetium-99m colloid uptake by the rat liver. J Nucl Med. 1988;29:1118–21.

Meckel's Diverticulum Study (Tc-99m-Pertechnetate)

39. Williams JG. Pertechnetate and the stomach: a continuing controversy. J Nucl Med. 1983;24:633–6.
40. Emamian SA, Shalaby-Rana E, Majd M. The spectrum of heterotopic gastric mucosa in children detected by Tc-99m pertechnetate scintigraphy. Clin Nucl Med. 2001;26:529–35.